INTERNATIONAL JOURNAL OF CONTROL
https://doi.org/10.1080/00207179.2021.1962968

Taylor & Francis
Taylor & Francis Group

Asymmetric delayed relay feedback identification based on the *n*-shifting approach

José Sánchez Moreno [a], Sebastián Dormido Bencomo [a], Oscar Miguel Escrig [b] and Julio Ariel Romero Pérez [b]

[a]Department of Computer Science and Automatic Control, Universidad Nacional de Educación a Distancia (UNED), Madrid, Spain; [b]Department of System Engineering and Design, Universitat Jaume I, Castelló de la Plana, Spain

ABSTRACT

The paper presents an improvement of the *n*-shifting technique to identify the frequency response of an industrial process using a fully asymmetric and delaying relay. The *n*-shifting approach allows the calculation of $n+1$ points of $G(s)$ by an asymmetric relay experiment. This set of n points is composed of $G(0)$, $G(j\omega_{osc}), \ldots, G(jn\omega_{osc})$, being ω_{osc} the oscillation frequency, and where $G(j\omega_{osc})$ is in most cases located in the third quadrant of the Nyquist map. By delaying the relay output and repeating a similar experiment it can be generated n additional points of $G(s)$ where the first point is $G(j\omega'_{osc})$ with $0 < \omega'_{osc} < \omega_{osc}$. In this way, it is possible to depict the full output spectrum of $G(s)$ from zero to very high frequencies by a short relay experiment. An example of identification and tuning of a PID controller with data from the *n*-shifting are presented to show the validity of the approach.

ARTICLE HISTORY
Received 15 October 2020
Accepted 27 July 2021

KEYWORDS
Asymmetric relay; estimation; system identification; oscillation

1. Introduction

Parametric and non-parametric relay-based feedback identification is a set of methods widely used in control engineering. From its origins in the 80's, the use of the describing function of a simple relay has been the most common of these methods to get the ultimate gain, frequency and phase lag of the process. With these data, it is possible to fit a first-order transfer function. If more information is required to fit a more complex model, additional experiments are necessary to force the system to oscillate at other frequencies to find additional points in the Nyquist map. Techniques to generate oscillations at lower frequencies than the original ω_{osc} are based on including additional time delays (Leva et al., 2006; Li et al., 1991; Scali et al., 1999; Tan et al., 1996), inserting an integrator (Friman & Waller, 1997; Sung & Lee, 2006; Wang & Shao, 1999), or modifying the hysteresis (Liu & Gao, 2012) or the asymmetry of the relay (Kishore et al., 2018). The original idea of this family of methods was proposed in a seminal paper by Åström & Hägglund, 1984. By using a delay or an integrator, the phase lag of the process is increased, and modifying the hysteresis, the negative reciprocal of the describing function of the relay is moved down along the negative axis of the Nyquist map.

However, as the describing function (DF) based methods give points in the Nyquist map whose accuracy depends on the filtering capacity of the process, other methods have been proposed based on different modifications of the Fourier transform (Cheon et al., 2010; Cheon et al., 2011; Ma & Zhu, 2006; Sung & Lee, 2000; Wang et al., 1997; Wang et al., 1999). All these algorithms have in common that they use all the process data from the initial transient region to the final cyclic steady-state part of the experiment. Such feature allows these algorithms to estimate points in the Nyquist map for any frequency going from 0 to the oscillation frequency ω_{osc} induced by the relay. With all these data it is possible to depict the spectrum of the process in this range of frequencies or to use some of them to estimate the parameters of a transfer function template. An interesting feature of these Fourier transform-based methods is that they only demand one relay-based experiment to generate the set of estimated points in the Nyquist map.

A method that allows obtaining two points in the Nyquist map is the 2-shifting method described in (Hofreiter, 2016, 2017, 2018; Hofreiter & Hornychová, 2019; Hornychová & Hofreiter, 2019). Through this procedure, it is possible to determine two points $G(j\omega_{osc})$ and $G(j2\omega_{osc})$ during one relay test by generating a second set of signals of frequency $2\omega_{osc}$ directly from $y(t)$ and $u(t)$. The generalisation of this method to obtain n points $G(jk\omega_{osc})$ $k = 1 \ldots n$ has been described in (Sánchez et al., 2021) and it is known as *n*-shifting method.; in such paper, some examples of process identification using the data provided by the *n*-shifting approach are described. This approach to estimate many points in one experiment constitutes the basis of the new scheme presented in this work.

The method presented in this paper allows estimating the full output spectrum of an unknown process $G(s)$ by combining a short relay experiment and the *n*-shifting approach. In (Sánchez et al., 2021), n points from ω_{osc} to $n\omega_{osc}$ are calculated in the experiment. In the approach presented in this paper, a set of n points from ω'_{osc} to $n\omega'_{osc}$ can be produced taking into account that $0 < \omega'_{osc} \leq \omega_{osc}$. So, the approach in (Sánchez et al., 2021) allows to study the system from a frequency ω_{osc}, corresponding to a point with a phase lag in the third quadrant

CONTACT José Sánchez Moreno jsanchez@dia.uned.es Department of Computer Science and Automatic Control, Universidad Nacional de Educación a Distancia (UNED), C/ Juan del Rosal 16, Madrid 28040, Spain

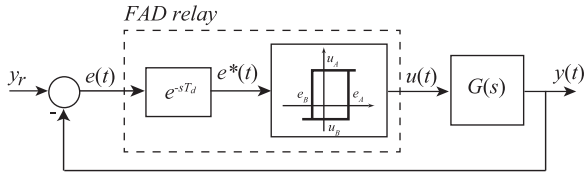

Figure 1. Configuration of the feedback control loop with a detailed view of the fully asymmetric and delaying relay.

[180°–270°] to high frequencies, while the approach described here captures the behaviour of the system at frequencies lower than ω_{osc} completing a full portrait of the output spectrum of the system.

The flexibility of the method is possible thanks to a fully asymmetric and delaying relay or FAD relay for short. Figure 1 presents the control scheme considered in this paper. The only difference with regard to a classical relay feedback control loop is that the FAD relay is biased in its input and output and can introduce a certain user-defined delay to its output. Modifying the biases and the delay, it is possible to change the initial oscillation frequency $\omega_{osc}$from which to start the estimation of the behaviour of the system at frequencies $n\omega_{osc}$ $n = 2, 3, 4, \ldots$ in each new experiment.

The paper is structured as follows. Section 2 is devoted to describing why and how the FAD relay can modify the behaviour of the system; to help explain it the describing function of the FAD relay will be calculated. Section 3 explains the n-shifting method to extract n points of $G(s)$ using the information stored in one oscillation period of $y(t)$ and $u(t)$. Although it is feasible to calculate the analytical expressions for relay feedback responses when the process is known (Panda & Yu, 2003), it is not possible to characterise the signals resulting from the shifting of $y(t)$ for a generic process because its dynamics is unknown. However, it is feasible for the relay because its input-output relationship is known beforehand but the result of the shifting applied to the relay output may not be very intuitive. For this reason, Section 4 presents a complete characterisation of the n-shifting approach applied to $u(t)$, which is a function of n and the FAD relay configuration. Section 5 describes different examples of the effectiveness of the method for estimating the full output spectrum of a process and of the tuning of a PID controller using the high accuracy of the estimation obtained by the n-shifting approach. Finally, some conclusions and further lines of work are given in Section 6.

2. The dual-input describing function of a fully asymmetric delaying relay

The describing function (DF) allows explaining theoretically the advantage that a FAD relay (see Figure 1) provides to estimate the spectrum response of a process.

Let us start with the fully asymmetric relay. The dual-input describing function (DIDF) approximation studies the sustained oscillations of a periodic wave with a bias, which is assumed to be $e^*(t) = B + A\sin(\omega t)$. This approximation characterises the behaviour of the non-linear part of a system with two different DFs (Gelb & Van der Velde, 1968), one related to the DC component B, which is the relation between input and output bias, and another one related to the oscillatory component of the input $A\sin(\omega t)$, which is the relation between the non-linearity output with regard to the sinusoidal input. The DF for the sinusoid is given by (see Appendix A):

$$N_A(A,B) = \frac{u_A - u_B}{\pi A}\left[\sqrt{1-\frac{(e_A-B)^2}{A^2}} + \sqrt{1-\frac{(e_B-B)^2}{A^2}}\right] - j\frac{(u_A-u_B)(e_A-e_B)}{\pi A^2} \quad (1)$$

and for the bias is given by

$$N_B(A,B) = \frac{(u_A+u_B)}{2B} + \frac{(u_A-u_B)}{2\pi B}\left[arcsin\frac{-e_B+B}{A} - arcsin\frac{e_A-B}{A}\right] \quad (2)$$

A and B are the amplitude of the first harmonic and the value of the bias, respectively. A is usually approximated by the limit cycle amplitude. It must be fulfilled that $A - |B| > \max(e_A, |e_B|)$ and B is calculated as

$$B = \frac{u_A+u_B}{2} + \frac{e_A+e_B}{2} \quad (3)$$

The DIDF, N_A, and N_B, provides necessary but not sufficient conditions for the existence of a limit cycle (Gelb & Van der Velde, 1968). As $G(s)$ is unknown but it is supposed to be operating in a limit cycle, from the conditions for the existence of oscillations it is only necessary to use this relation:

$$G(s) = -\frac{1}{N_A(A,B)} \quad (4)$$

This expression states that when there is an oscillation, an intersection of $G(s)$ with the negative reciprocal of N_A (critical locus) in the Nyquist map occurs. The intersection point is known as the critical point $G(j\omega_{osc})$, being ω_{osc} the frequency of the limit cycle. Figure 2 presents four configurations of the relay and the intersections of $-1/N_A$ with a process at two different frequencies. An increment of the hysteresis or horizontal asymmetry $HA = |e_A - e_B|$ produces a displacement of the horizontal line $-1/N_A$ along the vertical axis allowing to intersect with the process at lower frequencies. The modification of the vertical asymmetry, defined as $VA = |u_A - u_B|$, introduces a similar displacement plus an additional bending of $-1/N_A$. It must be noticed that when $VA = 0$, the bending effect disappears but the horizontal line can be moved down by decreasing u_A and $|u_B|$ even with $HA = 0$.

The other component of the FAD relay is the time delay T_d. As this phenomenon is linear, its DF is exactly its transfer function. So, we have

$$N_A = \cos\omega T_d - j\sin\omega T_d \quad (5)$$

The approximate DF of two series-connected nonlinearities can be computed directly by multiplication of the DFs of the individual nonlinearities. Such procedure assumes that the output of the first nonlinearity may be considered sinusoidal in

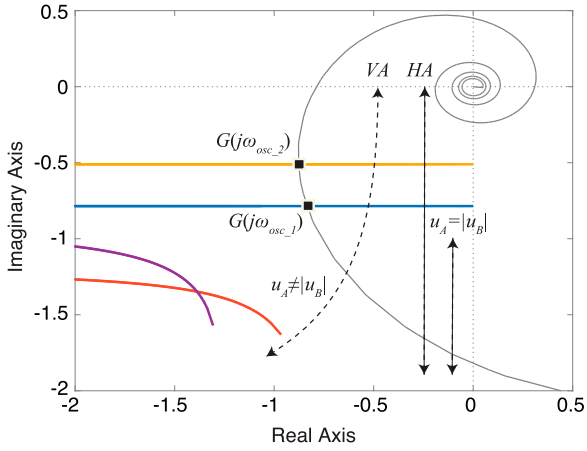

Figure 2. Example of the shift of $-1/N_A$ as a function of the relay asymmetry: fully symmetric (yellow), horizontal asymmetry (blue), vertical asymmetry (purple), fully asymmetric (red). The three dashed lines represent the effect that each type of asymmetry produces in $-1/N_A$. The transfer function is $G(s) = \frac{3e^{-0.5s}}{s+1}$.

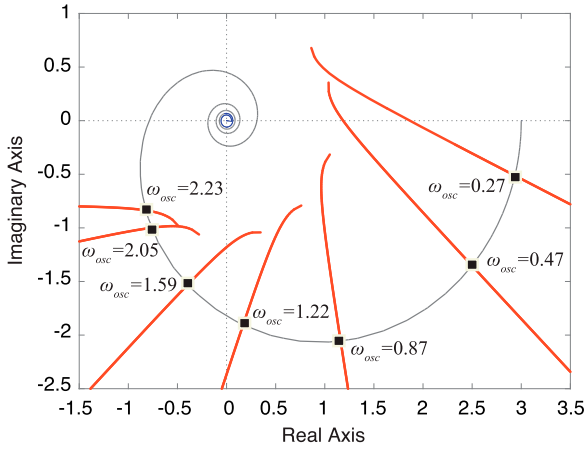

Figure 3. Examples of the counterclockwise rotation of $-1/N_A$ of the FAD relay as a function of the time delay for the FAD relay. $T_d = 0, 0.1, 0.5, 1, 2, 5$, and 10.

order to use the DF of the second nonlinearity in the subsequent overall calculation of the DF of two elements connected in series. Assuming the input is sinusoidal, the first component of the FAD relay, the time delay, produces a sinusoidal output that constitutes the input to the second nonlinearity, the asymmetric relay. So, the multiplication of the delay and the asymmetric relay DFs can be considered a good approximation for the calculation of the DF of the FAD relay.

Figure 3 presents an example of the counterclockwise rotation of the $-1/N_A$ of the FAD relay with a fully asymmetric setup and the same $G(s)$ as in Figure 2. It can be appreciated the effect that increasing the time delay has on the reduction of the frequency of the limit cycle generated. From a limit cycle at $\omega_{osc} = 2.23$ with $T_d = 0$, it can be reached another at $\omega_{osc} = 0.27$ if $T_d = 10$. It could be assumed that with a very high delay T_d, $-1/N_A$would be completely located in the first quadrant, meaning no oscillation because there is no intersection with $G(s)$. Actually, the drawing of $-1/N_A$ in the first quadrant happens but the oscillations exist, obviously at very low frequencies. The reason for this is that the process with very high T_d produces a nearly square signal as output, very far from

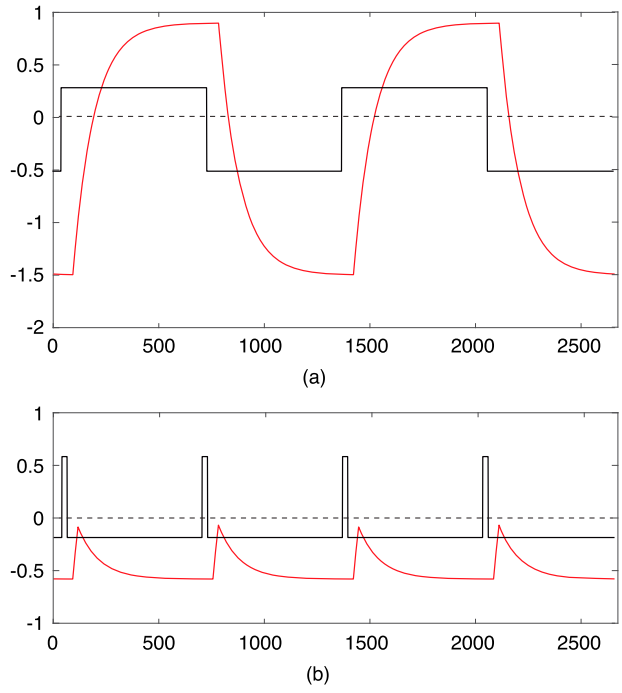

Figure 4. Waveforms of two cycles of $y(t)$ (red) and $u(t)$ (black) (upper plot) and their 2-shifting $y_2(t)$ (red) and $u_2(t)$ (lower plot).

a sinusoidal, existing a big discrepancy between the DF theory and the real situation.

3. Identification of $G(s)$ by the n-shifting technique

The n-shifting method is an extension of the original shifting approach that allows to generate a set of $N-1$ periodic signals $f_n(t)$ at frequencies $n\omega_{osc}$, $n = 2, 3, \ldots, N$, from a periodic signal $f(t)$ of frequency $\omega_{osc} = 2\pi/T$ with non-equal semi periods, that is, $T = T_1 + T_2$ and $T_1 \neq T_2$. The expression to calculate $f_n(t)$ from $f(t)$ is:

$$f_n(t) = \sum_{j=0}^{n-1} f\left(t - \frac{jT}{n}\right) = f(t) + f\left(t - \frac{T}{n}\right) + \ldots + f\left(t - \frac{(n-1)T}{n}\right) \quad (6)$$

where $n = 2, 3, \ldots, N$. These new signals are obtained by sums of the original signal and successive delayed copies. It must be noticed that the period of the new signal $f_n(t)$ is T/n.

If expression (6) is applied to a set of cycles of the signals $y(t)$ and $u(t)$ generated during a test with the FAD relay over a system G, it is possible to synthetise a set of N-1 signals $y_n(t)$ and $u_n(t)$ of frequencies $n\omega_{osc}$. Figure 4 shows the result of the n-shifting with $N = 2$ for the process $G(s) = \frac{3e^{-0.5s}}{s+1}$ using two cycles of $y(t)$ and $u(t)$ and the following FAD relay setup: $u_A = 0.3$, $u_B = -0.5$, $e_A = 0.5$, $e_B = -0.3$, $T_d = 5$. In this example, $\omega_{osc} = 0.473$ rad/s.

As it has been demonstrated in previous works (Hofreiter, 2016, 2017; Sánchez et al., 2021), the original 2-shifting technique and its n-shifting extension can be successfully applied to relay-feedback identification. The original signals $y(t)$ and $u(t)$

and the artificial $N-1$ $y_n(t)$ and $u_n(t)$ can be used to estimate $N+1$ points in the Nyquist map: $G(0)$, $G(j\omega_{osc})$, $G(j2\omega_{osc}), \ldots,$ $G(jN\omega_{osc})$.

In the following, it is explained how to obtain these points. Suppose that in a FAD relay feedback experiment at $t = t_s$, the system reaches a periodic stationary oscillation status and the period and frequency are T and ω_{osc}, respectively. Also, consider that the length of the signals $y(t)$ and $u(t)$ to get the Nyquist points by the n-shifting is limited to one full cycle. Once the data corresponding to a cycle are saved, the first step is to discount the effect of the additional delay of the FAD relay in the process output generating a new $y'(t)$.

This operation is done by rotating to the left the samples that compound the cycle of $y(t)$. Thus, if the sampling period is h, and $y(t) = [y_0, \ldots, y_{l-1}]$, then the rotation to the left to discount the delay is done by

$$y'(t) = [y_{d+1}, \ldots, y_{l-1}, y_0, \ldots, y_d] \tag{7}$$

where $d = T_d/h$. After that operation, the n-shifting can be correctly applied on the signals $y'(t)$ and $u(t)$ to synthetise the new signals $y'_n(t)$ and $u_n(t)$ by applying (6).

The following step is to calculate the Nyquist points. The Laplace transforms of the signals $y'(t)$ and $u(t)$ are:

$$Y'(s) = \frac{1}{1-e^{-Ts}} \int_0^T y'(t)e^{-st}dt \tag{8}$$

$$U(s) = \frac{1}{1-e^{-Ts}} \int_0^T u(t)e^{-st}dt \tag{9}$$

Therefore, the transfer function of $G(s)$ is

$$G(s) = \frac{Y'(s)}{U(s)} = \frac{\frac{1}{1-e^{-Ts}} \int_0^T y'(t)e^{-st}dt}{\frac{1}{1-e^{-Ts}} \int_0^T u(t)e^{-st}dt} = \frac{\int_0^T y'(t)e^{-st}dt}{\int_0^T u(t)e^{-st}dt} \tag{10}$$

Consequently, the process frequency response at ω_{osc} can be obtained by substituting s in (10) by $j\omega_{osc.}$. So, we get

$$G(j\omega_{osc}) = \frac{\int_0^T y'(t)e^{-j\omega_{osc}t}dt}{\int_0^T u(t)e^{-j\omega_{osc}t}dt} \tag{11}$$

Applying the same rationale to the signals derived from the n-shifting, we get

$$G(jn\omega_{osc}) = \frac{\int_0^{\frac{T}{n}} y'_n(t)e^{-jn\omega_{osc}t}dt}{\int_0^{\frac{T}{n}} u_n(t)e^{-jn\omega_{osc}t}dt} \tag{12}$$

The static gain is derived from (11) by setting $\omega_{osc} = 0$. So, we have

$$G(0) = \frac{\int_0^T y'(t)dt}{\int_0^T u(t)dt} \tag{13}$$

So, once the relay feedback experiment is running, the stationary oscillation has been reached and the value of ω_{osc} is measured, it is only necessary to process one cycle of $y(t)$ and $u(t)$. With these data and applying (11), (12) and (13), the $N+1$ points of $G(s)$ are estimated. Table 1 presented an excerpt of the code to make the n-shifting of a cycle of $y(t)$ and $u(t)$, including the discount of the effect of T_d.

3.1 On the selection of T_d

A convenient selection of T_d is key to improve the estimation of the full output spectrum of $G(s)$ from 0 to $N\omega_{osc}$. For example, the cycles presented in Figure 4 correspond to an experiment with $T_d = 5$ that produces a limit cycle at $\omega_{osc} = 0.473$ rad/s with $G(j\omega_{osc})$ presenting a phase lag of 40°; if the same experiment is run with $T_d = 0$, the limit cycle generated has $\omega_{osc} = 2.236$ rad/s and the phase lag of $G(j\omega_{osc})$ is 130°. With the second experiment, there is a range of points with a phase lag from 0° to 130° without information of their frequency response. Figure 5 presents the estimation of the output spectrum for the experiment described in the example of Figure 4 with $T_d = 5$; the number of points calculated by the n-shifting has been 39 ($N = 40$) providing a total of 41 points represented in the figure at frequencies 0, ω_{osc}, $2\omega_{osc}, \ldots, 40\omega_{osc}$.

The effect of T_d is explained by the rotation of the $-1/N_A$ of the FAD relay (see previous section). Higher values of T_d involve that the intersection with $G(s)$ will happen at lower frequencies. So, the higher T_d that the experiment can accept will allow accessing to lower frequencies.

However, determining the optimal value of T_d is a tricky issue because there is not a priori information of the process that is being estimated. A way to obtain a guess is by making an initial experiment with $T_d = 0$ and fitting a first-order plus time delay model $G_{FOPTD}(s) = G(0)e^{-Ls}/(Ts+1)$ by applying the following two expressions (Sánchez et al., 2018) once the initial experiment is finished,

$$T = \frac{\sqrt{G(0)^2 - |G(j\omega_{osc})|^2}}{\omega_{osc}|G(j\omega_{osc})|} \tag{14}$$

$$L = \frac{arg|G(j\omega_{osc})| + \arctan(\omega_{osc}T)}{\omega_{osc}} \tag{15}$$

With this FOPTD model, it is easy to estimate a value for T_d that will force the intersection of the $-1/N_A$ of the FAD relay with $G(s)$ near a low frequency $\omega'_{osc.}$ The expression to obtain the value is

$$argG_{FOPTD}(j\omega_{osc}) - argG_{FOPTD}(j\omega'_{osc}) = \omega'_{osc}T_d \tag{16}$$

The idea is to calculate the value of the delay that produces that the point $G(j\omega'_{osc})$ is rotated near to the area in the Nyquist map where the intersection with $-1/N_A$ of the FAD relay with $T_d = 0$ is produced, that is, to the point $G(j\omega_{osc})$. An example of the calculation of T_d by estimation of the model is presented in Example 2.

3.2 On the selection of N

If the n-shifting approach is used to generate points for fitting a transfer function, the approach must set to generate $N+1$ points where $N \geq M$, being M the order of the transfer function. However, if the approach is used to discover the output spectrum, a nice feature of the n-shifting approach is that the number of points of $G(s)$ to estimate can be done off-line, when the real experiment has finished. Once the samples corresponding to one stable cycle of $y(t)$ and $u(t)$ are saved, this information can be processed to generate $N+1$ points. If these points were

Table 1. Excerpt of the code that implements the *n*-shifting of a cycle of $y(t)$ and $u(t)$.

```
% Main variables
% dataY: One cycle of y(t).
% dataU: One cycle of u(t).
% h: Sampling period.
% n: Level of shifting.
% T1: Cycle of y(t) and u(t).
% wosc: Oscillation frequency.

%Discounting Td of y(t)

l = length(dataY);
delayTd = Td/h;
dataY = [dataY(delayTd+1:l-1) dataY(1:delayTd)];


% n-shifting of y(t) and u(t)

dataY_(1,:) = dataY;
dataU_(1,:) = dataU;

for i=2:n
     dataY_i = dataY;
     dataU_i = dataU;

     for j=2:i
          delay = round((j-1)*T1/(i*sampling));
          dataYd = [dataY(delay+1:l-1) dataY(1:delay+1)];
          dataUd = [dataU(delay+1:l-1) dataU(1:delay+1)];
          dataY_i = dataY_i + dataYd;
          dataU_i = dataU_i + dataUd;
     end
     dataY_(i,:) = dataY_i;
     dataU_(i,:) = dataU_i;
end

% Computation of G(0)

auxY =0; auxU =0;
for t=1:l
     auxY = auxY + dataY_(1,t);
     auxU = auxU + dataU_(1,t);
end
G0 = -auxY/auxU;

% Computation G(1), G(2), ..., G(n)

for j=1:n
     auxY = 0; auxU = 0; p = 0;

     for t=1:l
          p = p + h;
          auxY = auxY + dataY_(j,t)*exp(-1i*j*wos*p);
          auxU = auxU + dataU_(j,t)*exp(-1i*j*wos*p);
     end
     G(j) = -auxY/auxU;
end
```

not enough to cover the output spectrum, N can be increased and generate additional points at higher frequencies.

The computational effort to obtain the N points of the output spectrum must not be considered high because basically the *n*-shifting technique consists in rotating one cycle of $y(t)$ and $u(t)$ and making sums. Also, the job can be done off-line, once the experiment has finished and the data from one cycle are saved.

3.3 On the setup of the relay

The setup of the parameters e_A, e_B, u_A, and u_B can be more problematic because we do not have previous information of the process dynamics. Thus, it could be necessary to make preliminary tests in order to know the values that forces the system to oscillate using a symmetric setup, that is, $e_A = -e_B$ and $u_A = -u_B$. Once this configuration is known, it is necessary to set it in an asymmetric setup, that is, $e_A \neq -e_B$ and/or $u_A \neq -u_B$. Such configuration avoids that the sums of the semi periods for n odd in (12) and in (13) become zero. As a conclusion, if the relay is fully symmetric, it is only possible to obtain $G(jn\omega_{osc})$ with $n = 1, 3, 5, \ldots$ A byproduct result is that if $G(0) = \infty$ then $G(s)$ has integrators.

So, for example, if with $e_A = -e_B = \alpha$ and $u_A = -u_B = \beta$, the system enters in an oscillation when a set-point change is introduced, them $e_A > \alpha$ or/and $u_A > \beta$ would be a valid setup to apply the *n*-shifting.

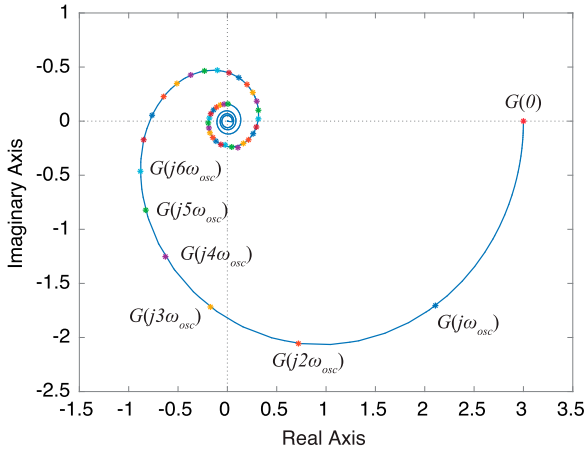

Figure 5. Estimation of the output spectrum of $G(s) = \frac{3e^{-0.5s}}{s+1}$. The continuous blue line represents the system; asterisks correspond to the 41 points estimated by the *n*-shifting but only the seven first ones have been labelled.

4. Characterisation of the *n*-shifting signals $u_n(t)$

It is interesting to analyse the possible waveforms $u_n(t)$ resulting from shifting the relay output $u(t)$. Now, it is known that any signal $u_n(t)$ resulting from the sum of $n-1$ delayed relay outputs $u(t)$, that can be expressed as

$$u_n(t) = \sum_{j=0}^{n-1} u\left(t - \frac{jT}{n}\right) = u(t) + u\left(t - \frac{T}{n}\right) + \ldots + u\left(t - \frac{(n-1)T}{n}\right) \quad (17)$$

is periodic. In this section, $u_n(t)$ is going to be characterised as a function of the relay hysteresis and the length of the summation n. To study that, let analyse the length of the semi periods of $u(t)$ that the asymmetric relay can produce depending on the hysteresis when its input is a sinusoidal signal of period T:

$$e^*(t) = \sin\left(\frac{2\pi}{T}t\right) \quad (18)$$

As the input signal is sinusoidal, the relationship between the switching times and the hysteresis limits is defined by

$$t_1 = \frac{T}{2\pi}\arcsin(e_A) \quad (19)$$

$$t_2 = \frac{T}{2} + \frac{T}{2\pi}\arcsin(|e_B|) \quad (20)$$

Without loss of generality, let consider the limits of the relay are $(-1, 1)$ in both axes. As the hysteresis values are within the ranges $0 < e_A < 1$ and $-1 < e_B < 0$, the switching times are bounded by the ranges $0 < t_1 < T/4$ and $T/2 < t_2 < 3T/4$, and the positive semi period will always satisfy that $T/4 < t_2 - t_1 < 3\,T/4$ (see Figure 6). So, we have

$$e_A \to 0 \Rightarrow t_1 \to 0 \qquad e_B \to 0 \Rightarrow t_2 \to \frac{T}{2}$$

$$e_A \to 1 \Rightarrow t_1 \to \frac{T}{4} \qquad e_B \to -1 \Rightarrow t_2 \to \frac{3T}{4}$$

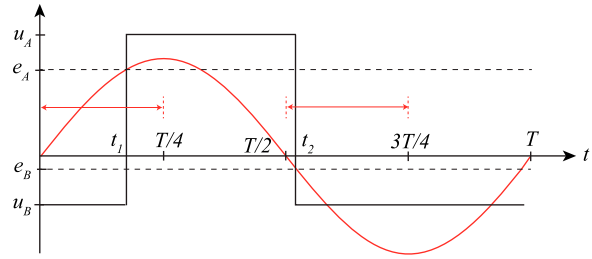

Figure 6. Example of the output signal (in black) of the asymmetric relay.

To characterise the waveforms that the summation (17) can generate it is necessary to analyse how the semi periods of the delayed signals overlap depending on the hysteresis and the delay applied.

Let us start by analysing the waveforms of $u_n(t)$ that can be obtained applying the shifting method when $n = 2$, that corresponds to a delay of $T/2$ and $u_2(t) = u(t) + u(t - T/2)$. So, there are three possible cases:

Case 1. $T/4 < t_2 - t_1 < T/2$. That situation corresponds to (Figure 7a). The result is a digital signal of frequency $T/2$ and amplitudes $2u_B$ and $u_A + u_B$.

Case 2. $T/2 < t_2 - t_1 < 3T/4$. It is obtained when $|e_A| > |e_B|$ (Figure 7b). The amplitudes are $u_A + u_B$ and $2u_A$.

Case 3. $t_2 - t_1 = T/2$. That corresponds to $|e_A| = |e_B|$. The shifting result is zero because $u(t) = -u\left(t - \frac{T}{2}\right)$.

So, in this case, the result of the 2-shifting can be two waveforms that change their amplitudes depending on the hysteresis.

When the *n*-shifting method is extended to $n = 3$, the resulting waveform is obtained by $\bar{u}(t) = u(t) + u(t - T/3) + u(t - 2T/3)$, that is, applying successive delays multiple of $T/3$ to the original relay output. Now, three are the situations that can be obtained by combining the relay constraint $T/4 < t_2 - t_1 < 3T/4$ and the delay $T/3$:

Case 1. $T/4 < t_2 - t_1 < T/3$ (Figure 8a). The waveform is a square signal of frequency $T/3$ and amplitudes $3u_A$ and $2u_A + u_B$ By some calculations, it is obtained that in this

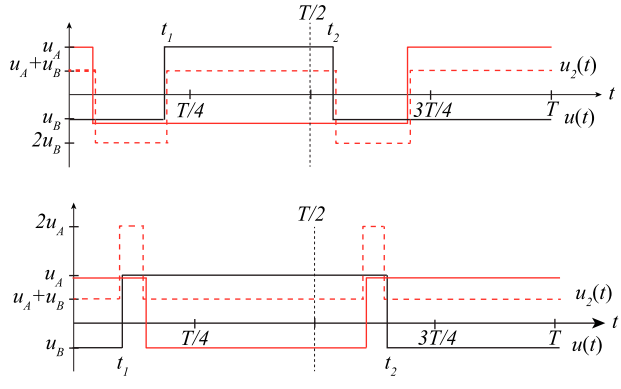

Figure 7. Possible $u_2(t)$ waveforms when the 2-shifting method is applied. The black line corresponds to $u(t)$, the continuous red line to $u(t - T/2)$, and the dashed red line to $u_2(t)$. (a) Case $T/4 < t_2 - t_1 < T/2$, (b) Case $T/2 < t_2 - t_1 < 3T/4$

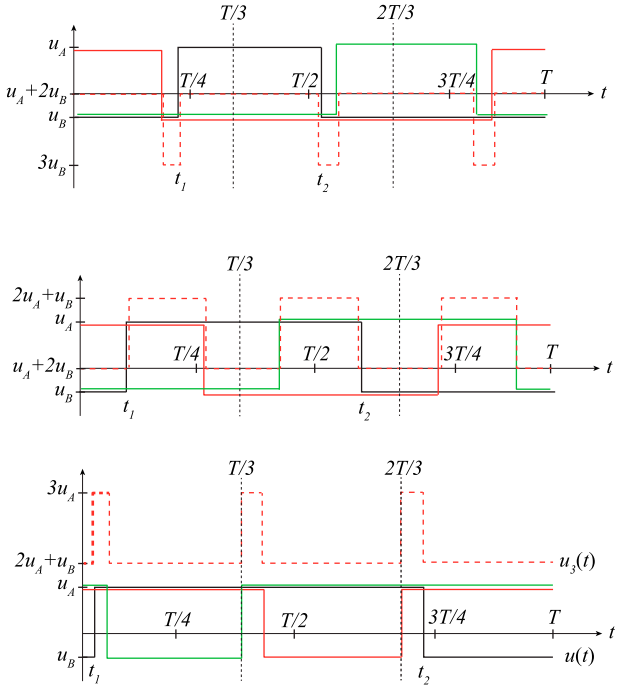

Figure 8. Possible $u_3(t)$ waveforms when the 3-shifting method is applied. The black line corresponds to $u(t)$, the continuous red line to $u(t - T/3)$, the continuous green line to $u(t - 2T/3)$, and the dashed red line to $u_3(t)$. (a) Case $T/4 < t_2 - t_1 < T/3$, (b) Case $T/3 < t_2 - t_1 < 2T/3$, (c) Case $2T/3 < t_2 - t_1 < 3T/4$.

case it is satisfied

$$e_A = -\frac{\sqrt{3}\sqrt{1-e_B^2}}{2} - \frac{e_B}{2}$$

Case 2. $T/3 < t_2 - t_1 < 2T/3$ (Figure 8b). The amplitudes are $2u_A + u_B$ and $u_A + u_B$. This case satisfies the following relationship:

$$-\frac{\sqrt{3}}{2} < -e_B\sqrt{1-e_A^2} - e_A\sqrt{1-e_B^2} < \frac{\sqrt{3}}{2}$$

Case 3. $2T/3 < t_2 - t_1 < 3T/4$ (Figure 8c). The amplitudes are $u_A + 2u_B$ and $3u_B$. The expression that is always fulfilled in this case is

$$\frac{\sqrt{3}\sqrt{1-e_B^2}}{2} - \frac{e_B}{2} = e_A$$

If $n = 4$, $u_4(t)$ is obtained by the summation of four periodic signals successively delayed multiples of $T/4$. Knowing that $0 < t_1 < T/4$ and $T/2 < t_2 < 3T/4$, the ranges for the positive semi period are two: $T/4 < t_2 - t_1 < 2T/4$ and $2T/4 < t_2 - t_1 < 2T/4$. The amplitudes of the two resulting binary waveforms are $2u_A + 2u_B$ and $u_A + 3u_B$, and $2u_A + 2u_B$ and $3u_A + u_B$, respectively. For the sake of brevity, the figures showing the two waveforms are not included.

Observing in Figures 7 and 8 the waveforms resulting from the n-shifting technique, it is possible to extrapolate the relationships between n and the number of resulting waveforms and their amplitudes. Table 2 shows these relationships from $n = 2$ to 8. According to this table, the possible $u_n(t)$ that the n-shifting approach can generate modifying the hysteresis of the relay is

$$N = 2\left(\frac{n-1}{4} + 1\right) - \sin\left(n\frac{\pi}{2}\right) \tag{21}$$

where x is the largest integer less than or equal to x.

Table 2. Examples of application of the n-shifting method.

Shifting N	Possible positive semi periods of $u(t)$ in relation to the delay T/n	Total of possible $u_n(t)$	Amplitudes of the semi periods of $u_n(t)$
2	$T/4 < t_2 - t_1 < T/2$ $T/2 < t_2 - t_1 < 3T/4$	2	$2u_A$ and $u_A + u_B$ $u_A + u_B$ and $2u_B$
3	$T/4 < t_2 - t_1 < T/4$ $T/3 < t_2 - t_1 < 2T/4$ $2T/3 < t_2 - t_1 < 3T/4$	3	$3u_A$ and $2u_A + u_B$ $2u_A + u_B$ and $3u_A$ $u_A + 2u_B$ $u_A + 2u_B$ and $3u_B$
4	$T/4 < t_2 - t_1 < 2T/4$ $2T/4 < t_2 - t_1 < 3T/4$	2	$3u_A + u_B$ and $2u_A + 2u_B$ $2u_A + 2u_B$ and $u_A + 3u_B$
5	$T/4 < t_2 - t_1 < 2T/5$ $2T/5 < t_2 - t_1 < 3T/5$ $3T/5 < t_2 - t_1 < 3T/5$	3	$4u_A + u_B$ and $2u_A + 3u_B$ $2u_A + 3u_B$ and $u_A + 4u_B$
6	$T/4 < t_2 - t_1 < 2T/6$ $2T/6 < t_2 - t_1 < 3T/6$ $3T/6 < t_2 - t_1 < 4T/6$ $4T/6 < t_2 - t_1 < 3T/4$	4	$5u_A + u_B$ and $4u_A + 2u_B$ $4u_A + 2u_B$ and $3u_A + 3u_B$ $3u_A + 3u_B$ and $2u_A + 4u_B$ $2u_A + 4u_B$ and $u_A + 5u_B$
7	$T/4 < t_2 - t_1 < 2T/7$ $2T/7 < t_2 - t_1 < 3T/7$ $3T/7 < t_2 - t_1 < 4T/7$ $4T/7 < t_2 - t_1 < 5T/7$ $5T/7 < t_2 - t_1 < 3T/4$	5	$6u_A + u_B$ and $5u_A + 2u_B$ $5u_A + 2u_B$ and $4u_A + 3u_B$ $4u_A + 3u_B$ and $3u_A + 4u_B$ $3u_A + 4u_B$ and $2u_A + 5u_B$ $2u_A + 5u_B$ and $u_A + 6u_B$
8	$T/4 = 2T/8 < t_2 - t_1 < 3T/8$ $3T/8 < t_2 - t_1 < 4T/8$ $4T/8 < t_2 - t_1 < 5T/8$ $5T/8 < t_2 - t_1 < 6T/8 = 3T/4$	4	$6u_A + 2u_B$ and $5u_A + 3u_B$ $5u_A + 3u_B$ and $4u_A + 4u_B$ $4u_A + 4u_B$ and $3u_A + 5u_B$ $3u_A + 5u_B$ and $2u_A + 6u_B$

The amplitudes of the semi periods of the N possible waveforms are defined by

$$\left(\frac{n+N}{2}-i\right)u_A+\left(n-\frac{n+N}{2}+i\right)u_B \text{ and}$$
$$\left(\frac{n+N}{2}-1-i\right)u_A+\left(n-\frac{n+N}{2}+1+i\right)u_B \quad (22)$$

with $i=0\ldots N-1$. The general idea is that to generate a new waveform $u_n(t)$, each cycle of $u(t)$ is divided into T/n sections and the overlapping of the delayed versions of $u(t)$ with $u(t)$ is produced in one of these sections depending on the value of t_2-t_1.

5. Examples

Next paragraphs are dedicated to explaining four examples of application of the n-shifting approach with the FAD relay: estimation of the output spectrum of a high-order process, guessing the T_d value, tuning of a PID controller, and analysis of the impact of measurement noise.

5.1 Example 1: estimation of the output spectrum of a high-order process

The first example corresponds to the following process

$$G_1(s)=\frac{1}{(s+1)^8} \quad (23)$$

previously used as case study in (Ma & Zhu, 2006; Wang et al., 1997, 1999). Before starting the experiment, the FAD relay setup was fixed to $e_A=0.5$, $e_B=-0.3$, $u_A=0.6$, $u_B=-0.6$, and $T_d=0$ and the N value in the n-shifting approach was set to 15 to estimate 16 points. The oscillation frequency generated in the experiment with such relay setup was $\omega_{osc}=0.287$.

Figure 9a,b present the 15 signals obtained by applying the n-shifting to two full cycles of the signals $y(t)$ and $u(t)$. It seems in Figure 10a that the signals from $y_7(t)$ to $y_{15}(t)$ correspond to a stationary but it is not true; the signals are really oscillating but their amplitudes are very low to be appreciated.

Figure 9c shows the Nyquist plot with the 16 points estimated by the n-shifting approach and the red line depicting the $-1/N_A$. It can be seen the difference between the theoretical critical point corresponding to the intersection of $-1/N_A$ and $G_1(s)$ with the critical point corresponding to $G_1(j\omega_{osc})$ that represents the real oscillation of the system. In this example, the signal $y(t)$ is very sinusoidal so the discrepancy between the theoretical critical point defined by the DF and the real one is very close. The points from $G_1(j5\omega_{osc})$ to $G_1(j15\omega_{osc})$ are not visible in Figure 9c because they are concentrated in the high-frequency area of the curve and they overlapped.

Figure 10 presents a similar experiment with the same process but considerably increasing T_d, for instance to 40, to identify frequencies below the oscillation frequency of the previous experiment, that is $\omega_{osc}=0.287$. It can be noticed in Figure 10a the new position of $-1/N_A$ in the Nyquist plot thanks to T_d. In this new experiment, the system oscillates at $\omega_{osc}=0.0617$ and the discrepancies between the theoretical critical point and the real critical point are high, which is a consequence of the form of the signal $y(t)$ that is far from resembling a sinusoid and is closer to a square signal (see Figure 10b).

As said before, it is important to notice that the value of N can be fixed when the experiment has concluded, and the signals $y(t)$ and $u(t)$ have been saved. It is only necessary to store the samples corresponding to one stable cycle of both signals to apply the n-shifting approach. The only limitation to fix N is determined by the number of samples that compound one cycle of $y_N(t)$ and $u_N(t)$. Each time that new signals $y_n(t)$ and $u_n(t)$ are calculated by (6), the number of samples that compound the cycle of the signals is reduced and the accuracy of the integrations in (11) can became compromised.

So, if a cycle of $y(t)$ and $u(t)$ is formed by M samples, one cycle of $y_N(t)$ and $u_N(t)$ will count with M/N samples. The relationship between M and N must be high enough to guarantee that the number of samples in (11) allows integrating with accuracy.

In the two study cases of Example 1, one cycle of $y(t)$ and $u(t)$ is composed approximately by 4500 and 10,000 samples (see Figures 9a and 10b). That means that for $N=15$, one cycle of $y_{15}(t)$ and $u_{15}(t)$ is formed by 4500/15 = 300 samples and 10,000/15 = 666.66 samples in each case. These amounts of samples are reasonable to calculate $G_1(j15\omega_{osc})$ with accuracy in both cases.

5.2 Example 2: making a guess of T_d by a FOPTD model

In this example, it is described how to estimate a value for $T_d$based on a FOPTD model of the real process following the procedure explained in Section 3.1. The process chosen is

$$G_2(s)=\frac{1}{(s+1)^4} \quad (24)$$

and the configuration of the relay for an initial experiment in order to fix T_d is

$$e_a=0.5, e_b=-0.5, u_a=1, u_b=-0.8, T_d=0$$

After running a first experiment and applying the shifting approach to one cycle of $u(t)$ and $y(t)$, the following values were measured

$$w_{osc}=0.59\,\text{rad/s}$$

$$G_2(0)=0.999699$$

$$G_2(jw_{osc})=-0.293756-0.464535j$$

With these values, the following FOPTD model was obtained

$$G_{FOPTD}(s)=\frac{0.999}{2.5767\text{s}+1}e^{-1.9392s} \quad (25)$$

Let suppose that we want to know the output spectrum of $G_2(s)$ from $\omega'_{osc}=0.1$ rad/s. By applying (16)

$$argG_{FOPTD}(j0.59)-argG_{FOPTD}(j0.1)=0.1T_d \quad (26)$$

it is obtained $T_d=17$. Running a new experiment but with $T_d=17$, the oscillation frequency is lower than the original one, that is, $\omega_{osc}=0.1403$ rad/s, near to the pursued $\omega'_{osc}=0.1$.

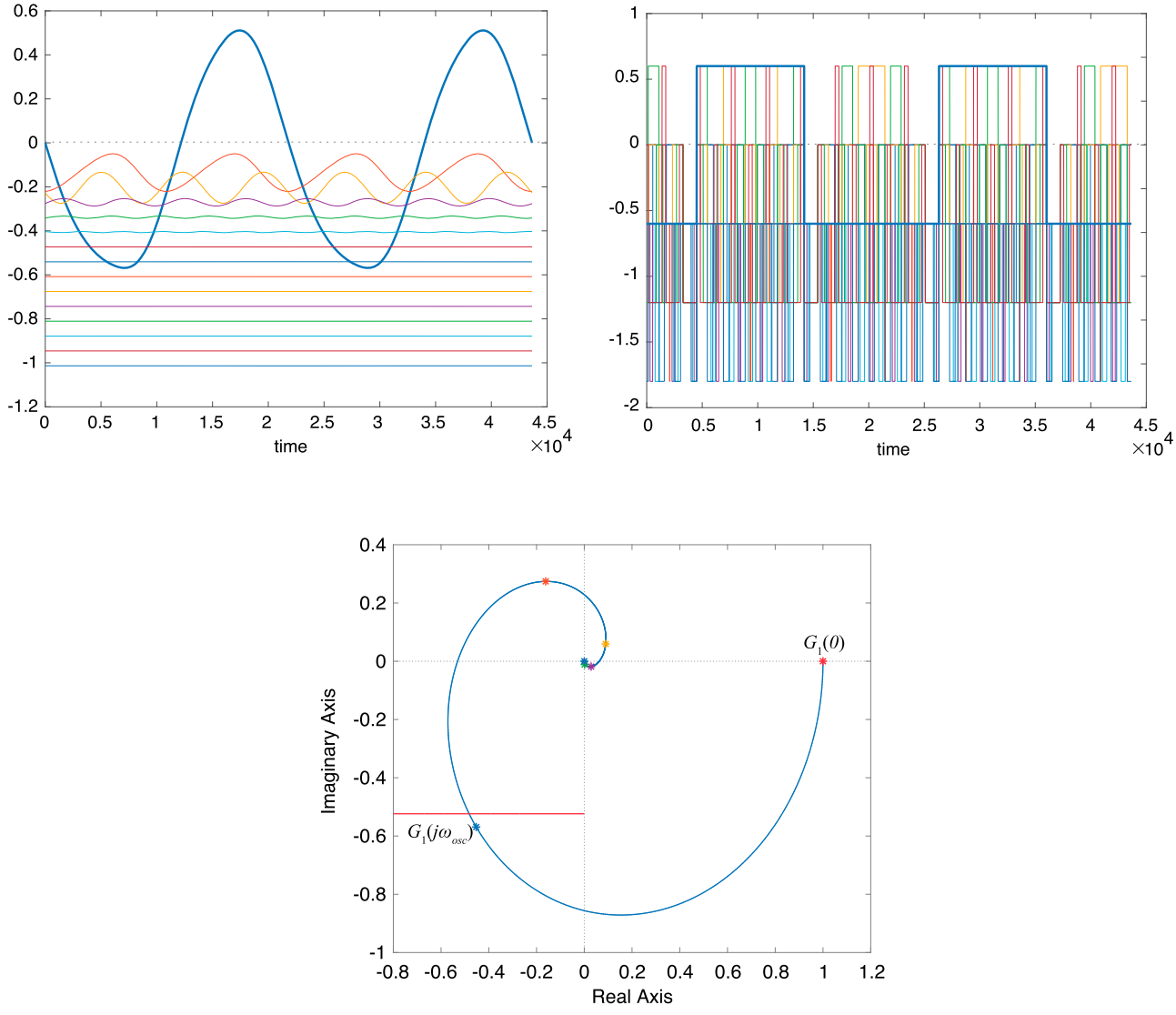

Figure 9. (a) and (b) Waveforms obtained by the *n*-shifting of two cycles of $y(t)$ and $u(t)$ (thick blue lines) from the experiment corresponding to the estimation of $G_1(s) = (s+1)^{-8}$. (c) Nyquist plot of $G_1(s)$ with the 16 points estimated from the waveforms obtained by *n*-shifting.

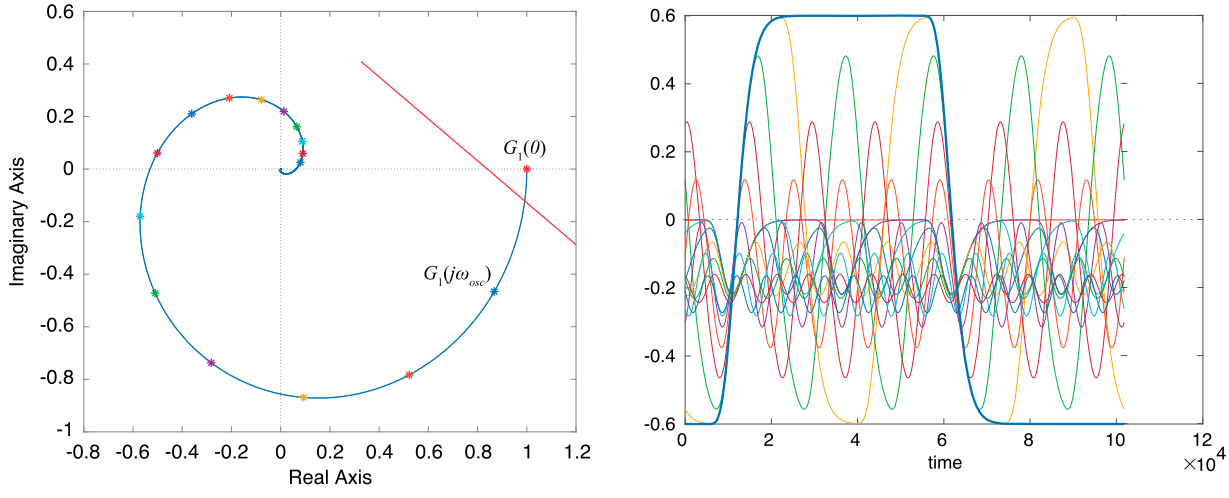

Figure 10. (a) Nyquist plot of $G_1(s) = (s+1)^{-8}$ with the estimated points obtained by fixing $T_d = 40$ in the FAD relay. (b) Waveforms obtained by the *n*-shifting of one cycle of $y(t)$ (thick blue line).

If a lower frequency is necessary, for example $\omega'_{osc} = 0.01$ rad/s, applying (16) it is obtained $T_d = 200$. Now, running another experiment with this T_d, the oscillation frequency obtained is $\omega_{osc} = 0.015$ rad/s. As a conclusion, the method based on a FOPTD model can be considered good enough to obtain a guess of T_d.

5.3 Example 3: tuning of a PID controller

The following example is focused on presenting the advantage of exploiting the accurate estimation of the n-shifting approach for the tuning of an PID controller using genetic algorithms (GAs).

The procedure followed in this example has been (a) to estimate the output spectrum of an unknown process by the n-shifting approach; (b) to generate a N-order transfer function with the points obtained from the n-shifting, and (c) to tune a PID controller by an evolutionary algorithm using the N-order model with the goal, for example, of minimising the integrated absolute error (IAE) after a set-point change. After that, the performance has been compared and contrasted with another PIDs tuned with the GA but using the real process and reduced-order models, for instance, FOPTD and SOPTD models

Consider the following process studied in the literature (Kaya & Atherton, 2001; Liu & Gao, 2012; Wang et al., 1997).

$$G_3(s) = \frac{e^{-0.5s}}{(s^2 + s + 1)(s + 1)} \tag{27}$$

The configuration of the FAD relay chosen for the experiment is

$$e_a = 0.5, e_b = -0.5, u_a = 1, u_b = -0.8, T_d = 0$$

where the T_d parameter has been fixed to zero because knowing information from the low frequencies range located in the fourth quadrant of the Nyquist map is not relevant for our tuning purposes.

After running the experiment, and as indicated in Subsection 3.2, the n-shifting approach is set to generate $N + 1$ points where $N \geq M$, being M the order of the transfer function to fit. Without loss of generality, in this example, a stable 10-order system is estimated using the *tfest* function from the System Identification Toolbox of Matlab/Simulink to gather all the dynamics of the unknown process. Thus, the transfer function estimated by *tfest* is

$$G_{tfest}(s) = \frac{1.137 \cdot 10^6}{\begin{array}{c} s^{10} + 15.65\, s^9 + 335\, s^8 + 3621\, s^7 + 3.4 \cdot 10^4\, s^6 \\ +2.154 \cdot 10^5 s^5 + 9.75 \cdot 10^5\, s^4 + 2.67 \cdot 10^6\, s^3 \\ +3.63 \cdot 10^6\, s^2 + 2.87 \cdot 10^6\, \mathrm{s} + 1.13 \cdot 10^6 \end{array}} \tag{28}$$

Figure 11 shows the Nyquist plot of the real process, the high-order model using the 10 points from the n-shifting approach, and the FOPTD and SOPTD models fitted by other relay feedback identification approaches presented in (Kaya & Atherton, 2001; Liu & Gao, 2012; Sánchez et al., 2018; Wang et al., 1997),

$$G_{S'a\ nchez}(s) = \frac{e^{-2.126s}}{0.814s + 1} \tag{29}$$

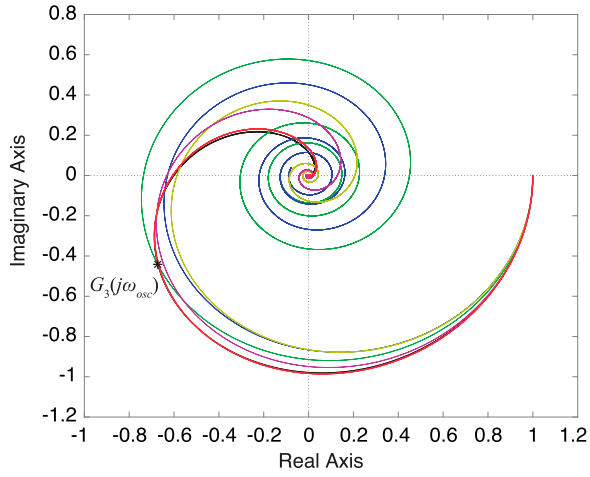

Figure 11. Nyquist plots of $G_3(s)$ (black) and the five models estimated by different relay feedback identification methods: G_{tfest} (red), $G_{Sánchez}$ (green), G_{Wang} (blue), G_{Kaya} (yellow), G_{Liu} (magenta).

$$G_{Wang}(s) = \frac{e^{-2.1s}}{1.152s + 1} \tag{30}$$

$$G_{Kaya}(s) = \frac{e^{-1.633s}}{(0.785s + 1)^2} \tag{31}$$

$$G_{Liu}(s) = \frac{e^{-1.3105s}}{0.9744s^2 + 1.4194s + 1} \tag{32}$$

It can be appreciated in Figure 11 that the dynamics of the real process $G_3(s)$ is gathered by the high-order model G_{tfest} (the plot of $G_3(s)$ is nearly overlapped by the G_{tfest} model) and the differences existing with the low-order models, specially at high frequencies.

Once the high-order model was estimated, the tuning of the PID controller for the real process and the five models is done by using a GA with the objective of minimising the IAE after a set-point change. The GA was run using the *ga* function from the Global Optimization Toolbox of Matlab with a population size of 30. The simulation time for running the simulation of the system in each generation of the GA was fixed to 150s. Also, the space of search of K_p, T_i and T_d was fixed to [0.001, 10], [0.1, 500], and [0.1, 50], respectively.

Table 3 presents the results of the tuning and the IAE for the six systems. It can be appreciated in Table 3 that the set of parameters more similar to the obtained from tuning the real process with the GA corresponds to the model G_{tfest}, fitted with the points obtained from the n-shifting approach.

Table 3. Comparative of PID tuning parameters and *IAE*.

Process	K_p	T_i	T_d	*IAE*
G_3	1.0439	2.3181	1.2985	2.7319
G_{tfest}	0.9933	2.2760	1.3005	2.7931
$G_{Sánchez}$	0.5942	1.8168	0.6024	3.170
G_{Wang}	0.7281	2.2202	0.6518	3.2156
G_{Kaya}	0.8084	2.3499	0.7642	3.1302
G_{Liu}	0.7838	2.0851	0.9669	2.9298

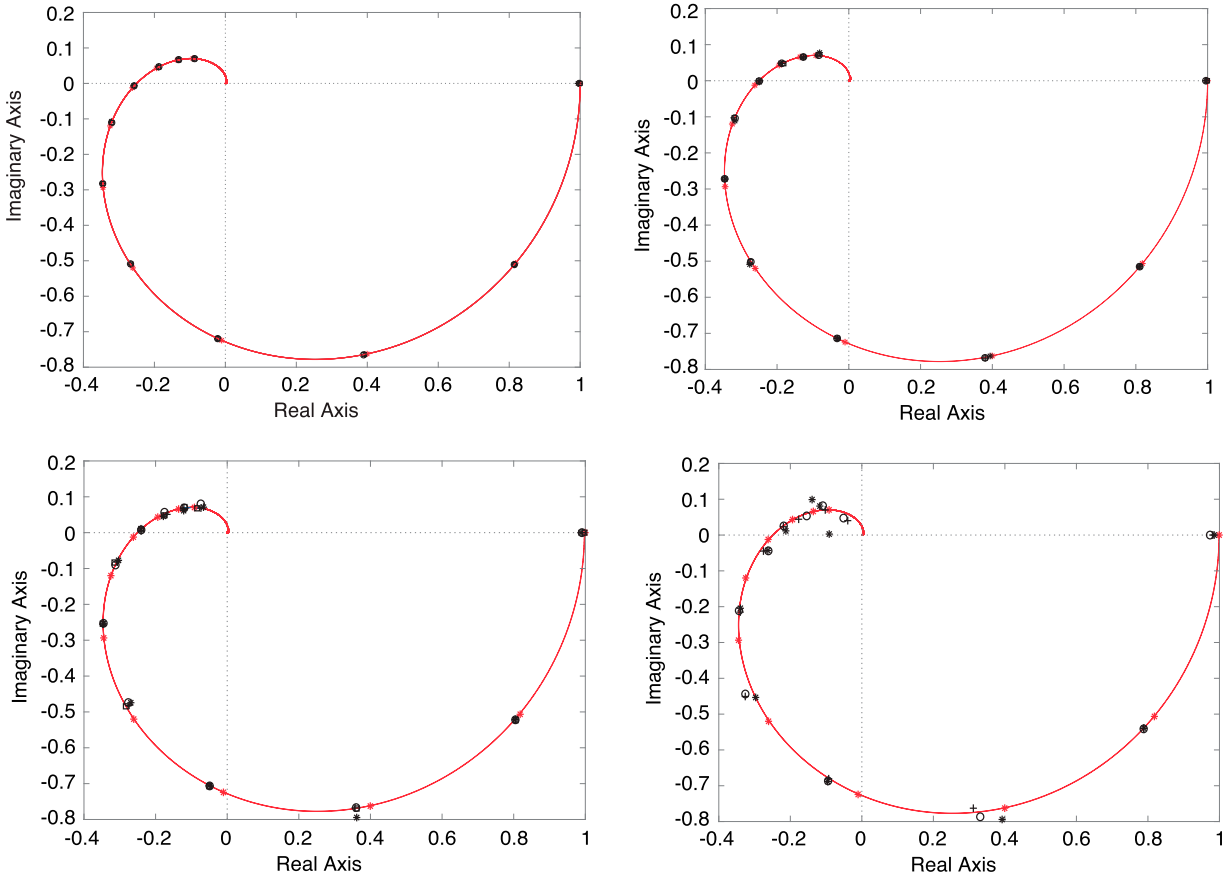

Figure 12. Nyquist plot of $G_2(s)$ and points estimated by n-shifting with different levels of noise: 5% (a), 10% (b), 20% (c), and 50% (d). Legend: without noise (red $*$), 1 cycle (black $*$), 3 cycles (black o), 6 cycles (black $+$), and 10 cycles (black ■).

5.4 Example 4: effect of the measurement noise

One of the advantages of the FAD relay is that the hysteresis band $\delta = e_A - e_B$ reduces the influence of the measurement noise n_0 avoiding by false switching and producing a noiseless control action when the level of noise is not very high. However, the process output is not free of noise and in presence of relevant measurement noise would be convenient a previous filtering of the process output because the signals $y_n(t)$ are synthetised by the n-shifting of $y(t)$, and the influence of noise would be transmitted to them. If there was not filtering of $y(t)$ or n_0 was not fully removed, the n-shifting could be applied using more than one cycle of the signals $y(t)$ and $u(t)$ to reduce the noise mean value.

To analyse how the noise affects the results and how using more than one cycle in the n-shifting could reduce the influence of noise, a set of experiments have been conducted for the balanced process used in the Example 2, that is, $G_2(s) = \frac{1}{(s+1)^4}$. To introduce noise in the simulations, band-limited white noise was connected to the process output with different amplitudes, $n_0 = [0.05\delta, 0.1\delta, 0.2\delta, 0.5\delta]$. The configuration of the FAD relay was fixed to full asymmetry with a T_d value to access to the low-frequency range of the spectrum (see Example 2),

$$e_a = 0.6, e_b = -0.4, u_a = 1, u_b = -0.8, T_d = 17, N = 10$$

With such setting, the n-shifting approach was applied increasing the number of cycles used of $y(t)$ and $u(t)$ to apply the expressions (6), (7), (11) and (12). Figure 12 presents the results.

A noise level of 5% and 10% does not deteriorate the accuracy of the estimates regardless the number of cycles used. However, it can be appreciated that a noise level of 20% already introduces small discrepancies in the results but if the level of noise is increased to 50%, the values are not acceptable.

After examining the results in Figure 12, the conclusion is that the number of cycles of $y(t)$ and $u(t)$ used for applying the n-shifting approach does not improve the estimations and that the approach can cope with levels of noise lower than 10% without filtering the signals.

6. Conclusions

An approach for the estimation of the output spectrum of an unknown system has been presented in this paper. The method is based on inserting a FAD relay in a feedback loop and run an experiment to put the system to oscillate. Once the system has reached a stable limit cycle, the data corresponding to one cycle of the signals $y(t)$ and $u(t)$ are processed by the n-shifting approach to generate the output spectrum.

The advantage of the n-shifting for identification appears really when the transfer functions to fit is of a high order, for example N, and $N+1$ points of $G(s)$ must be estimated from one experiment. It allows the fitting of a stable model of the order necessary to gather the dynamics of the real process and

take advantage of such fact by using, for example, an evolutionary algorithm as PID tuning procedure. Also, the insertion of the FAD relay allows to improve the approach by forcing $G(s)$ to oscillate at lower frequencies than using a simple asymmetric relay. In this way, the output spectrum of the system that can be discovered in one experiment is much more complete because the range of frequencies analysed can start at frequencies near zero.

The main issue detected is to establish a relationship between the time delay T_d of the FAD relay and the frequency of the oscillation; and it is difficult because the system is unknown. A way to solve such issue is by making a first experiment with $T_d = 0$ and fitting a simple first-order plus time delay model; with this model, it is easy to suggest a value for the time delay that will force the intersection of the $-1/N_A$ of the FAD relay with $G(s)$ at the desired frequency.

Further lines of work are oriented to extend this approach to an event-based PI context using as event-based sampler a symmetric send-on-delta strategy.

Disclosure statement

No potential conflict of interest was reported by the author(s).

Funding

This work was supported by MINECO: [grant number DPI2017-84259-C2-2-R, RTI2018-094665-B-I00]; Ministerio de Ciencia e Innovación: [grant number TEC2015-69155-R]; CEIE, Generalitat Valenciana: [grant number ACIF/2018/244]; Universitat Jaume I: [grant number 18I411-Uji-b2018-39].

ORCID

José Sánchez Moreno http://orcid.org/0000-0002-6702-3771
Sebastián Dormido Bencomo http://orcid.org/0000-0002-2405-8771
Oscar Miguel Escrig http://orcid.org/0000-0002-2472-2038
Julio Ariel Romero Pérez http://orcid.org/0000-0003-3397-2239

References

Åström, K. J., & Hägglund, T. (1984). Automatic tuning of simple regulators with specifications on phase and amplitude margins. *Automatica*, *20*(5), 645–651. https://doi.org/10.1016/0005-1098(84)90014-1

Cheon, Y. J., Jeon, C. H., Lee, J., Lee, D. H., & Sung, S. W. (2010). Improved Fourier transform for processes with initial cyclic-steady-state. *AIChE Journal*, *56*(6), 1536–1544. https://doi.org/10.1002/aic.12068

Cheon, Y. J., Sung, S., Lee, J., Cheol, J., & In-Beum, L. (2011). Improved frequency response model identification method for processes with initial cyclic-steady-state. *AIChE Journal*, *57*(12), 3429–3435. https://doi.org/10.1002/aic.12550

Friman, M., & Waller, K. V. (1997). A two-channel relay for autotuning. *Industrial and Engineering Chemical Research*, *36*(7), 2662–2671. https://doi.org/10.1021/ie970013u

Gelb, A., & Van der Velde, W. E. (1968). *Multiple-input describing functions and nonlinear system design*. McGraw-Hill.

Hofreiter, M. (2016). Shifting method for relay feedback identification. *IFAC-PapersOnLine*, *49*(12), 1933–1938. https://doi.org/10.1016/j.ifacol.2016.07.913

Hofreiter, M. (2017). Biased-relay feedback identification for time delay systems. *IFAC-PapersOnLine*, *50*(1), 14620–14625. https://doi.org/10.1016/j.ifacol.2017.08.1740

Hofreiter, M. (2018). Alternative identification method using biased relay feedback. *IFAC-PapersOnLine*, *51*(11), 891–896. https://doi.org/10.1016/j.ifacol.2018.08.491

Hofreiter, M., & Hornychová, A. (2019). *Process identification using relay shifting method for autotuning of PID controller*. Proceedings of the MATEC web of conference, vol. 292.

Hornychová, A., & Hofreiter, M. (2019). *Shifting method for relay feedback identification implemented in PLC tecomat*. Proceedings of the 20th international carpathian control conference (ICCC).

Kaya, I., & Atherton, D. P. (2001). Parameter estimation from relay autotuning with asymmetric limit cycle data. *Journal of Process Control*, *11*(4), 429–439. https://doi.org/10.1016/S0959-1524(99)00073-6

Kishore, D., Anand Kishore, K., & Panda, R. C. (2018). Identification and control of process using the modified asymmetrical relay feedback method. *Procedia Computer Science*, *133*, 1029–1034. https://doi.org/10.1016/j.procs.2018.07.072

Leva, A., Bascetta, L., & Schiavo, F. (2006). Model-based proportional–integral/ proportional–integral–derivative (PI/PID) autotuning with fast relay identification. *Industrial and Engineering Chemical Research*, *45*(12), 4052–4062. https://doi.org/10.1021/ie051311r

Li, W., Eskinat, E., & Luyben, W. L. (1991). An improved autotune identification method. *Industrial and Engineering Chemical Research*, *30*(7), 1530–1541. https://doi.org/10.1021/ie00055a019

Liu, T., & Gao, F. (2012). *Industrial process identification and control: Design step-test and relay-experiment-based methods*. Springer-Verlag.

Ma, M., & Zhu, X. (2006). A simple auto-tuner in frequency domain. *Computers and Chemical Engineering*, *30*(4), 581–586. https://doi.org/10.1016/j.compchemeng.2005.09.004

Panda, R. C., & Yu, C. C. (2003). Analytical expressions for relay feedback responses. *Journal of Process Control*, *13*(6), 489–501. https://doi.org/10.1016/S0959-1524(02)00119-1

Sánchez, J., Dormido, S., & Díaz, J. M. (2021). Fitting of generic process models by an asymmetric short relay feedback experiment: The *n*-shifting method. *Applied Sciences*, *11*(4), 1651. https://doi.org/10.3390/app11041651

Sánchez, J., Guinaldo, M., Dormido, S., & Visioli, A. (2018). Enhanced event-based identification procedure for process control. *Industrial and Engineering Chemical Research*, *57*(21), 7218–7231. https://doi.org/10.1021/acs.iecr.7b05239

Scali, C., Marchetti, G., & Semino, D. (1999). Relay with additional delay for identification and autotuning of completely unknown processes. *Industrial and Engineering Chemical Research*, *38*(5), 1987–1997. https://doi.org/10.1021/ie980616l

Sung, S. W., & Lee, I. B. (2000). An improved algorithm for automatic tuning of PID controllers. *Chemical Engineering Science*, *55*(10), 1883–1891. https://doi.org/10.1016/S0009-2509(99)00455-8

Sung, S. W., & Lee, J. (2006). Two-channel relay feedback method under static disturbances. *Industrial and Engineering Chemical Research*, *45*(12), 4071–4074. https://doi.org/10.1021/ie0513393

Tan, K. K., Lee, T. H., & Wang, Q. G. (1996). An enhanced automatic tuning procedure for PI/PID controllers for process control. *AIChE Journal*, *42*(9), 2555–2562. https://doi.org/10.1002/aic.690420916

Wang, Q. G., Chang-Chida Hang, C. C., & Bi, Q. (1997). Process frequency responses estimation from relay feedback. *Control Engineering Practice*, *5*(9), 1293–1302. https://doi.org/10.1016/S0967-0661(97)84368-7

Wang, Q. G., Chang-Chida Hang, C. C., & Bi, Q. (1999). A technique for frequency response identification from relay feedback. *IEEE Transactions on Control Systems Technology*, *7*(1), 122–128. https://doi.org/10.1109/87.736766

Wang, Y., & Shao, H. (1999). PID autotuner based on gain- and phase-margin specifications. *Industrial and Engineering Chemical Research*, *38*(8), 3007–3012. https://doi.org/10.1021/ie9808007

Appendix A: Calculation of the DIDF of a fully asymmetric relay

Let consider the asymmetric relay presented in Figure 1 whose input waveform $x(t) = B + A\sin\varphi$ is composed of a sinusoid plus a bias. Analysing the output waveform generated by the relay (see Figure A1), we know

$$e_A = B + A\sin\phi_1 \Rightarrow \phi_1 = \arcsin\frac{e_A - B}{A} \tag{A1}$$

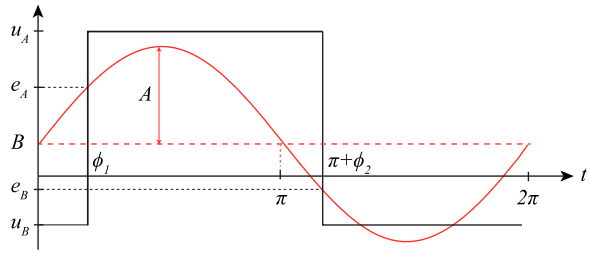

Figure A1. Input and output waveforms for the asymmetric relay.

$$e_B = B - A\sin\phi_2 \Rightarrow \phi_2 = \arcsin\frac{-e_B + B}{A} \tag{A2}$$

The DIDF of an asymmetric relay consists of two gains (Gelb & Van der Velde, 1968) defined as

$$N_B(A,B) = \frac{1}{2\pi B}\int_0^{2\pi} y(\varphi)d\varphi \tag{A3}$$

$$N_A(A,B) = \frac{j}{\pi A}\int_0^{2\pi} y(\varphi)e^{-j\varphi}d\varphi \tag{A4}$$

A.1 Calculation of $N_B(A,B)$

From (A3)

$$\begin{aligned} N_B(A,B) &= \frac{1}{2\pi B}\int_0^{2\pi} y(\varphi)d\varphi = \frac{1}{2\pi B}\int_0^{2\pi} y(B + A\sin\varphi\,)d\varphi \\ &= \frac{1}{2\pi B}\left[\int_0^{\phi_1} u_B d\varphi + \int_{\phi_1}^{\pi+\phi_2} u_A d\varphi + \int_{\pi+\phi_2}^{2\pi} u_B d\varphi\right] \\ &= \frac{1}{2\pi B}[\phi_1 u_B + (\pi + \phi_2 - \phi_1)u_A + (\pi - \phi_2)u_B] \\ &= \frac{u_A + u_B}{2B} + \frac{u_A - u_B}{2\pi B}(\phi_2 - \phi_1) \end{aligned} \tag{A5}$$

Substituting (A1) and (A2) in (A5), we obtain the final expression

$$N_B(A,B) = \frac{(u_A + u_B)}{2B} + \frac{(u_A - u_B)}{2\pi B}\left[arcsin\frac{-e_B + B}{A} - arcsin\frac{e_A - B}{A}\right] \tag{A6}$$

A.2 Calculation of $N_A(A,B)$

$$\begin{aligned} N_A(A,B) &= \frac{j}{\pi A}\int_0^{2\pi} y(\varphi)e^{-j\varphi}d\varphi = \frac{j}{\pi A}\int_0^{2\pi} y(B + A\sin\varphi)e^{-j\varphi}d\varphi \\ &= \frac{j}{\pi A}\left[\int_0^{\phi_1} u_B e^{-j\varphi}d\varphi + \int_{\phi_1}^{\pi+\phi_2} u_A e^{-j\varphi}d\varphi + \int_{\pi+\phi_2}^{2\pi} u_B e^{-j\varphi}d\varphi\right] \\ &= \frac{j}{\pi A}[u_B j e^{-j\varphi}|_0^{\phi_1} + u_A j e^{-j\varphi}|_{\phi_1}^{\pi+\phi_2} + u_B j e^{-j\varphi}|_{\pi+\phi_2}^{2\pi}] \\ &= \frac{j}{\pi A}[u_B j(e^{-j\phi_1} - 1) + u_A j(e^{-j(\pi+\phi_2)} - e^{-j\phi_1}) \\ &\quad + u_B j(e^{-j2\pi} - e^{-j(\pi+\phi_2)})] \\ &= \frac{j}{\pi A}[u_B j(\cos\phi_1 - j\sin\phi_1 - 1) + u_A j(\cos(\pi + \phi_2) \\ &\quad - j\sin(\pi + \phi_2) - \cos\phi_1 + j\sin\phi_1) \\ &\quad + u_B j(\cos 2\pi - j\sin 2\pi - \cos(\pi + \phi_2) + j\sin(\pi + \phi_2))] \\ &= \frac{-1}{\pi A}[u_B(\cos\phi_1 - j\sin\phi_1 - 1) \\ &\quad + u_A(-\cos\phi_2 + j\sin\phi_2 - \cos\phi_1 + j\sin\phi_1) \\ &\quad + u_B(1 + \cos\phi_2 - j\sin\phi_2)] \\ &= \frac{-1}{\pi A}[u_B(\cos\phi_1 - 1) + u_A(-\cos\phi_2 - \cos\phi_1) \\ &\quad + u_B(1 + \cos\phi_2)] \\ &\quad - \frac{j}{\pi A}[-u_B\sin\phi_1 + u_A(\sin\phi_2 + \sin\phi_1) - u_B\sin\phi_2] \\ &= \frac{-1}{\pi A}[u_B(\cos\phi_1 + \cos\phi_2) - u_A(\cos\phi_2 + \cos\phi_1)] \\ &\quad - \frac{j}{\pi A}[-u_B(\sin\phi_1 + \sin\phi_2) + u_A(\sin\phi_2 + \sin\phi_1)] \end{aligned} \tag{A7}$$

From (A1) and (A2), we know

$$\sin\phi_1 = \frac{e_A - B}{A} \Rightarrow \cos\phi_1 = \sqrt{1 - \frac{(e_A - B)^2}{A^2}} \tag{A8}$$

$$\sin\phi_2 = \frac{-e_B + B}{A} \Rightarrow \cos\phi_2 = \sqrt{1 - \frac{(e_B - B)^2}{A^2}} \tag{A9}$$

Applying (A7) and (A8) to (A6), we obtain

$$\begin{aligned} N_A(A,B) &= \frac{u_A - u_B}{\pi A}\left[\sqrt{1 - \frac{(e_A - B)^2}{A^2}} + \sqrt{1 - \frac{(e_B - B)^2}{A^2}}\right] \\ &\quad - \frac{j}{\pi A}(u_A - u_B)\left[\frac{e_A - B}{A} - \frac{e_B - B}{A}\right] \end{aligned} \tag{A10}$$

and reordering the terms, we get the final expression

$$\begin{aligned} N_A(A,B) &= \frac{u_A - u_B}{\pi A}\left[\sqrt{1 - \frac{(e_A - B)^2}{A^2}} + \sqrt{1 - \frac{(e_B - B)^2}{A^2}}\right] \\ &\quad - j\frac{(u_A - u_B)(e_A - e_B)}{\pi A^2} \end{aligned} \tag{A11}$$

When drawing $-\frac{1}{N_A}(A,B)$ in a Nyquist plot, it is necessary to fix the initial value A to avoid the imaginary values that can appear from the square roots of (A11). Observing the two square roots, the value of B must be fixed from the relay setting. This d.c. gain in the relay output can be estimated from the asymmetric setup as

$$B = \frac{u_A + u_B}{2} + \frac{e_A + e_B}{2}$$

So, substituting B in the two inequalities obtained from the square roots in (A11)

$$1 - \frac{(e_A - B)^2}{A^2} \geq 0$$

$$1 - \frac{(e_A - B)^2}{A^2} \geq 0$$

Solving the inequalities, the range of valid values of A is $(A_{\min}, \infty)$, where

$$A_{\min} = \max\left(\frac{e_A - e_B - u_A - u_B}{2}, \frac{e_A - e_B + u_A + u_B}{2}\right)$$